

Microwave Field Emission

E. Tanabe, A. McEuen, M. Trail, G. Meddaugh and S. Bandy

Varian Associates, Inc.
911 Hansen Way
Palo Alto, California 94304-1028

ABSTRACT

A demountable S-band single-cavity test fixture designed to study the influence of surface materials and processing techniques on microwave field-emission is described. Results for polycrystalline and single crystal copper (machined/polished and electro-discharge machined) as well as molybdenum samples are presented.

INTRODUCTION

Microwave field-emission is detrimental to high gradient accelerator operation, since it can absorb a significant portion of the available rf power as well as produce unwanted beam and x-ray radiation. Moreover, it may induce voltage breakdown which can interrupt operation and possibly damage the structure. On the other hand, controlled microwave field-emission from a metallic cold cathode would make possible a high current density, low-emittance electron-beam source for application in high power tubes, accelerators and microwave switches. Interest in both these aspects has prompted efforts to understand and develop techniques to control microwave field-emission (REF: 1,2,3).

This paper describes a demountable, single cavity field-emission tester which was developed and tested to study the macroscopic geometrical field-enhancement factor β and the dependence of microwave field-emission on material, surface finishes, temperature, pulse-width, repetition rate, pressure level, rf processing, poisoning agents and cavity surface treatment (including coatings of various materials). The modified Fowler-Nordheim plots obtained are presented and discussed. A limited number of results are available at the present time. The program, however, is continuing and further results will be reported in future papers.

EXPERIMENTAL SET-UP AND PROCEDURE

Measurements were made in a test fixture consisting of one-half of a typical high-gradient accelerator cavity, shown in Figure 1. Field emission of electrons occurs from the outside radius of the nose surrounding the beam hole, where the highest voltage gradients exist. Therefore, in this cavity the nose was made removable, so that the effects of material and

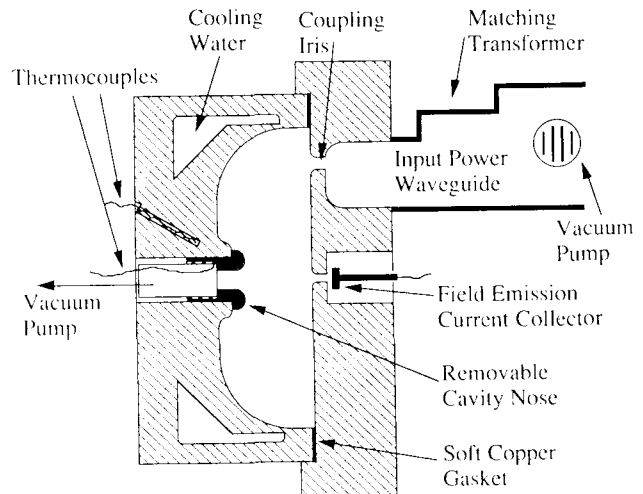


Fig. 1 - Schematic of Field Emission Test Cavity.

surface finish could be determined. The test cavity was clamped to a flat shorting plate at what would be the central plane of symmetry of a full accelerator cavity. The distance from the nose tip to the shorting plate is 1.85 cm. Both cavity and shorting plate were made of oxygen-free high-conductivity (OFHC) copper and were cooled by circulating water. A gasket of annealed copper was used as a vacuum and rf seal at their junction. The field-emission current collector was placed behind a 0.2 cm diameter, radiused hole in the shorting plate directly opposite the nose. RF power was introduced into the cavity through a smoothly radiused coupling iris near the periphery, matched to standard WR284 waveguide by a two-step quarter-wave transformer. The test system was isolated from the pressurized input waveguide by a ceramic disk window and was maintained at a pressure level of 10^{-7} torr by ion pumps in the input waveguide and through the center hole of the cavity nose. For each experiment the test nose, a new gasket, the cavity, and the surface of the shorting plate were carefully degreased and rinsed with acetone and deionized water. The parts were then assembled and pumped down to the 10^{-7} torr level, which was maintained during a 12-hour bake-out at 200°C.

With each nose installed, the room-temperature low-power cavity resonant frequency (~ 2996 MHz), input VSWR

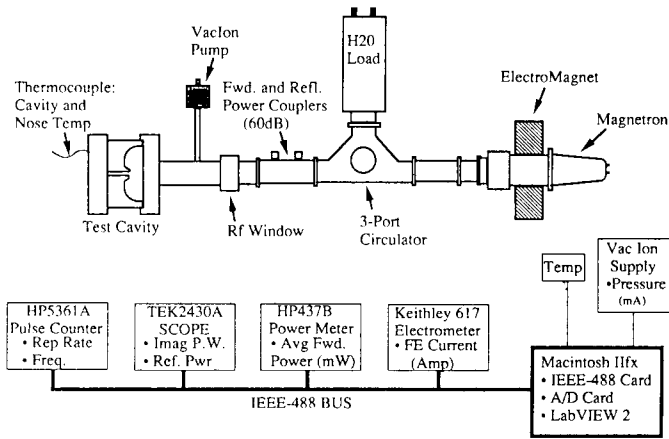


Fig. 2 - Field Emission Tester RF System and Instrumentation Schematic.

(typically $1.1:1$), and cold Q_0 (9,500-10,000) were measured.

High-power tests were performed with the equipment set-up shown in Figure 2. Power was generated by a tunable magnetron which was isolated from the cavity by a circulator. Incident and reflected power were measured via calibrated 60 dB directional couplers in the waveguide near the window. Peak power was varied from 0.2 to 2.0 MW by varying the magnetic field and anode voltage of the magnetron. RF pulse-width was 4.5 μsec , and pulse repetition rate was varied between 100 and 300 pps, yielding an average power level of 0.09 to 2.7 kW. The cooling water which circulated through the cavity body and the shorting plate was maintained at $40 \pm 5^\circ\text{C}$. Thermocouples were attached to the nose insert and to the body of the cavity for monitoring the temperature rise during high-power test. The cavity pressure level was estimated by measuring the vac-ion pump current. After rf processing, data were taken at a fixed repetition rate as the peak power was increased from a low level to just below the breakdown threshold. Tests were repeated in a 100-200-300 pps repetition rate sequence until stable results indicated that the surface was well-conditioned.

An automated instrumentation system, incorporating a Macintosh IIfx and LabVIEW 2 software, was used for rapid and accurate data collection and presentation. The system, shown in Figure 2, automatically collected the required data and recorded it on the Macintosh via the IEEE-488 Bus and A/D card. Vac-ion pressure, cavity temperature and nose temperature were monitored through the A/D card.

EXPERIMENTAL RESULTS

Figure 3 shows the typical variation of measured (time-averaged) field-emission current with the peak rf surface field

(E_0) on a machined, diamond-polished OFHC nose. The threshold level of E_0 for initiating field-emission in an S-band cavity is about 100MV/m, while the breakdown threshold level is about 250MV/m. No hysteresis was observed as E_0 was increased and decreased.

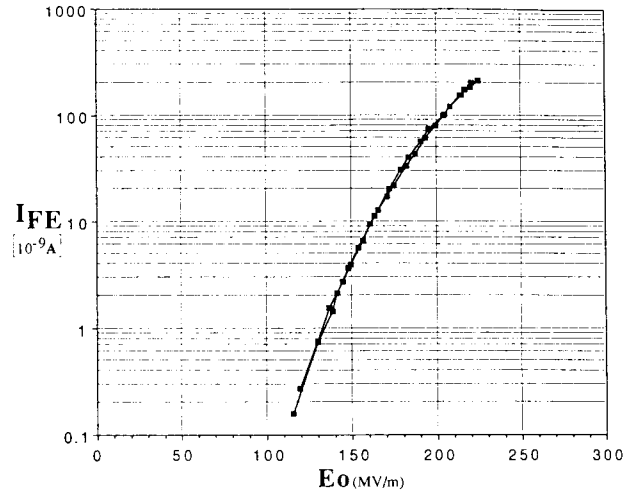


Fig. 3 - Typical Field Emission vs. Electric Field Curve for a machined, diamond-polished OFHC copper nose.

Figure 4 shows the detected field-emission current and rf field waveforms within the test cavity. The field-emission current rises slowly to its maximum value (1.5 μsec), but falls off very rapidly (0.6 μsec).

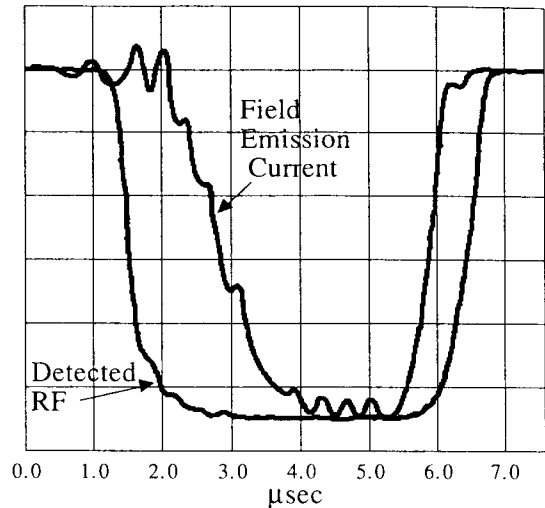


Fig. 4 - Field Emission and rf field waveforms.

Figure 5 shows the modified Fowler-Nordheim results for a machined, diamond-polished OFHC nose as a function of rf processing. The β value dropped from an initial value of 58 to 45 after approximately 18 hours of processing. Once the β reached a value of 45 additional processing did not seem to produce further improvement.

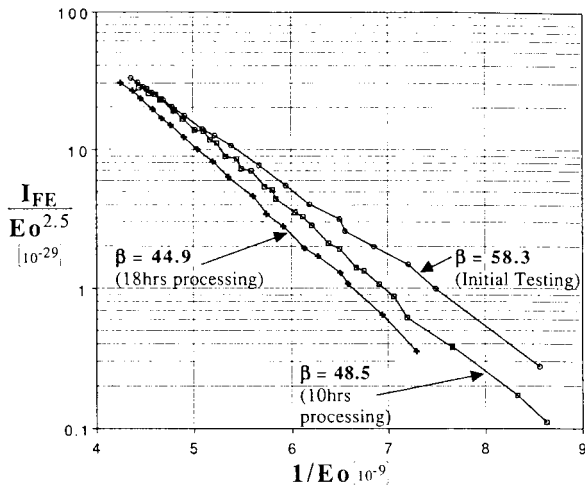


Fig. 5 - Fowler-Nordheim Plots at initial testing and after 18hrs continuous processing. Machined, diamond-polished OFHC copper nose.

At higher field-emission current levels the Q of the cavity decreased, due to an increase in the effective beam-loading of the cavity. This effect can be determined by measuring the reflection coefficient at higher power levels. The measured, unloaded Q dropped from a low-power value of 9700 to 8500 for a peak surface field of 230 MV/m. The corresponding power loss was 0.2 MW compared to the total input power of 1.8 MW.

Figure 6 shows the Fowler-Nordheim results for various materials and surface finishing techniques. Chemical polishing can usually minimize, if not eliminate, mechanical defects

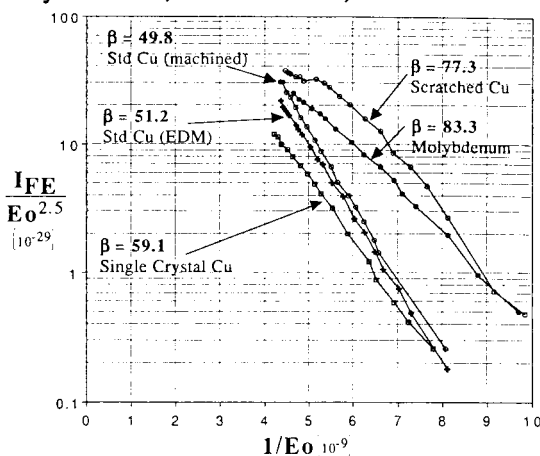


Fig 6 - Typical Fowler-Nordheim Curves: Machined, diamond-polished Cu, EDM-Etched Cu, Single Crystal (EDM-Etched), Molybdenum (machined).

such as burrs and scoring, which are typically left by machining and subsequent mechanical polishing. However, it usually enhances the sharp edges at the grain boundaries due to the relative differences in etch rates of the adjacent, randomly-ori-

ented crystallites. Electro-discharge machining (EDM) can minimize these effects, as well as the formation of dislocations caused by machining. Therefore, the use of a single-crystal material in combination with EDM finishing should produce the smoothest microscopic surface possible.

The results show that both field-emission current level and β (~50) are very similar for EDMed and mechanically-polished copper. The single crystal copper produced a slightly higher β than polycrystalline copper but resulted in reduced field-emission current (~50% lower at high E_0). Molybdenum had a high β (~83) and higher field-emission current at lower electric-field levels. The scratched nose (machined copper purposely scarred) resulted in a high β (~77) and the highest recorded field-emission current.

CONCLUSION

A test system capable of evaluating β and field-emission characteristics of various materials has been successfully developed and tested. Test results appear to indicate that there is a lower limit to β . Improvements to the surface microstructure by polishing, EDM machining and use of single-crystal copper provide little improvement beyond the β threshold of ~50. Since the geometric field-enhancement can only account for a β of approximately 10, the high values of β obtained must be due to other factors. Possible explanations are surface contaminants, hot electron emission through a dielectric layer, and surface polymerization by impinging electrons or x-rays. Future tests are planned to explore some of these possibilities.

Conclusions that have been made in this paper are based on results collected to date and are preliminary.

ACKNOWLEDGMENTS

The authors wish to thank Nick Cortese and Frank Gordon who helped develop the test system and conduct the tests.

REFERENCES

- [1] G.A. Loew and J.W. Wang "Field Emission and RF Breakdown in Copper Linac Structures" SLAC-PUB-5059, Aug., 1989
- [2] S. Takeda, M. Akemoto, H. Hayano, H. Matsumoto, and T. Naito "High Gradient Experiment by the ATF", 1991 IEEE Proceedings of Particle Accelerator Conference, pp2061-2063.
- [3] J.W. Wang, "RF Properties of Periodic Accelerating Structures for Linear Colliders", SLAC-Report-339, July 1989, Ph.D. Dissertation.